THE JOURNAL OF BIOLOGICAL CHEMISTRY VOL. 283, NO. 46, pp. 31726–31735, November 14, 2008


# Structural Interactions between Transmembrane Helices 4 and 5 of Subunit *a* and the Subunit *c* Ring of *Escherichia coli* ATP Synthase*

Received for publication, May 19, 2008, and in revised form, August 14, 2008 Published, JBC Papers in Press, September 11, 2008, DOI 10.1074/jbc.M803848200

**Kyle J. Moore and Robert H. Fillingame**[1]

*From the Department of Biomolecular Chemistry, School of Medicine and Public Health, University of Wisconsin, Madison, Wisconsin 53706*

**Subunit *a* plays a key role in promoting $H^+$ transport and the coupled rotary motion of the subunit *c* ring in $F_1F_0$-ATP synthase. $H^+$ binding and release occur at Asp-61 in the middle of the second transmembrane helix (TMH) of $F_0$ subunit *c*. $H^+$ are thought to reach Asp-61 via aqueous pathways mapping to the surfaces of TMHs 2–5 of subunit *a*. TMH4 of subunit *a* is thought to pack close to TMH2 of subunit *c* based upon disulfide cross-link formation between Cys substitutions in both TMHs. Here we substituted Cys into the fifth TMH of subunit *a* and the second TMH of subunit *c* and tested for cross-linking using bis-methanethiosulfonate (bis-MTS) reagents. A total of 62 Cys pairs were tested and 12 positive cross-links were identified with variable alkyl length linkers. Cross-linking was achieved near the middle of the bilayer for the Cys pairs *a*248C/*c*62C, *a*248C/*c*63C, *a*248C/*c*65C, *a*251C/*c*57C, *a*251C/*c*59C, *a*251C/*c*62C, *a*252C/*c*62C, and *a*252C/*c*65C. Cross-linking was achieved near the cytoplasmic side of the bilayer for Cys pairs *a*262C/*c*53C, *a*262C/*c*54C, *a*262C/*c*55C, and *a*263C/*c*54C. We conclude that both *a*TMH4 and *a*TMH5 pack proximately to *c*TMH2 of the *c*-ring. In other experiments we demonstrate that *a*TMH4 and *a*TMH5 can be simultaneously cross-linked to different subunit *c* monomers in the *c*-ring. Five mutants showed pH-dependent cross-linking consistent with *a*TMH5 changing conformation at lower pH values to facilitate cross-linking. We suggest that the pH-dependent conformational change may be related to the proposed role of *a*TMH5 in gating $H^+$ access from the periplasm to the *c*Asp-61 residue in *c*TMH2.**

The $F_1F_0$-ATP synthases of oxidative phosphorylation utilize the energy of a transmembrane electrochemical gradient of $H^+$ or $Na^+$ to mechanically drive the synthesis of ATP via two coupled rotary motors in the $F_1$ and $F_0$ sectors of the enzyme (1–3). In the intact enzyme, ATP synthesis or hydrolysis takes place in the $F_1$ sector at the surface of the membrane, synthesis being coupled to $H^+$ transport through the transmembrane $F_0$ sector. Homologous enzymes are found in mitochondria, chloroplasts, and many bacteria (4). In *Escherichia coli* and other eubacteria, $F_1$ consists of five subunits in an $\alpha_3\beta_3\gamma\delta\epsilon$ stoichiometry (4). $F_0$ is composed of three subunits in a likely ratio of $a_1b_2c_{10}$ in *E. coli* and *Bacillus subtilis* PS3 or $a_1b_2c_{11}$ in the $Na^+$ translocating *Ilyobacter tartaricus* ATP synthase (3, 5–7), and may contain as many as 15 *c* subunits in other bacterial species (8). Subunit *c* spans the membrane as a helical hairpin with the first TMH[2] on the inside and the second TMH on the outside of the *c*-ring (7, 9, 10). A high resolution x-ray structure of the *I. tartaricus* $c_{11}$-ring has revealed the sodium binding site at the periphery of the ring with chelating groups to the bound $Na^+$ extending from two interacting subunits (7). The essential *I. tartaricus* Glu-65 in the $Na^+$ chelating site corresponds to *E. coli* Asp-61. In the $H^+$-transporting *E. coli* enzyme, Asp-61 at the center of the second TMH is thought to undergo protonation and deprotonation as each subunit of the *c* ring moves past a stationary subunit *a*. In the complete membranous enzyme, the rotation of the *c* ring is proposed to be driven by $H^+$ transport at the subunit *a*/*c* interface, with ring movement then driving rotation of subunit $\gamma$ within the $\alpha_3\beta_3$ hexamer of $F_1$ to cause conformational changes in the catalytic sites leading to synthesis and release of ATP (1–3).

Subunit *a* folds in the membrane with 5 TMHs and is thought to provide aqueous access channels to the proton-binding Asp-61 residue on the *c*-ring (11–14). Interaction of the conserved Arg-210 residue in *a*TMH4 with *c*TMH2 is thought to be critical during the deprotonation-protonation cycle of *c*Asp-61 (14–17). Previously, we probed Cys residues introduced into the 5 TMHs of subunit *a* for aqueous accessibility based upon their reactivity with $Ag^+$ (18–20). Two regions of aqueous access were found with distinctly different properties. One region in TMH4, extending from Asn-214 and Arg-210 at the center of the membrane to the cytoplasmic surface, contains Cys residues that are sensitive to inhibition by NEM and $Ag^+$. A second set of $Ag^+$-sensitive and NEM-insensitive residues mapped to the opposite face and periplasmic side of *a*TMH4. $Ag^+$-sensitive and NEM-insensitive residues extending from the center of the membrane to the periplasmic surface were also found in TMHs 2, 3, and 5.

Little is known about the structure or three-dimensional arrangement of the TMHs in subunit *a*. Based initially upon the

* This work was supported, in whole or in part, by National Institutes of Health Grant GM23105. The costs of publication of this article were defrayed in part by the payment of page charges. This article must therefore be hereby marked "*advertisement*" in accordance with 18 U.S.C. Section 1734 solely to indicate this fact.

[1] To whom correspondence should be addressed: 1300 University Ave., Madison, WI 53706. Tel.: 608-262-1439; Fax: 608-262-5253; E-mail: rhfillin@wisc.edu.

[2] The abbreviations used are: TMH, transmembrane helix; bis-MTS, bis-methanethiosulfonate; βMSH, β-mercaptoethanol; M2M, 1,2-ethanediyl *bis*-MTS; M3M, 1,3-propanediyl bis-MTS; M4M, 1,4-butanediyl *bis*-MTS; M6M, 1,6-hexanediyl bis-MTS; PVDF, polyvinylidene difluoride; DTT, dithiothreitol; NEM, *N*-ethylmaleimide; PBS, phosphate-buffered saline.

position of several sets of second site suppressor mutations, we recently introduced pairs of Cys into putatively apposing TMHs and tested for zero-length cross-linking with disulfide bond formation catalyzed by $Cu^{2+}$ (21). Cross-links were found with eight different Cys pairs and define a juxtaposition of TMHs 2–3, 2–4, 2–5, 3–4, 3–5, and 4–5 packing in a proposed four-helix bundle (21). The $Ag^{+}$-sensitive and NEM-insensitive residues in TMHs 2, 3, 4, and 5 cluster at the interior of the predicted four-helix bundle, and could interact to form a continuous aqueous pathway extending from the periplasmic surface to the center of the membrane (14, 20, 21). In the cross-linking supported model, the NEM-sensitive residues in TMH4 pack on the peripheral face and cytoplasmic side of the four-helix bundle (14, 18). $Cu^{2+}$-catalyzed cross-links were also observed between Cys pairs introduced into *a*TMH4 and *c*TMH2 (22). Seven high yield cross-links were identified over a span of 19 amino acids, *i.e.* a span that would nearly traverse the bilayer. The cross-linkable faces of these helices would include Asp-61 in *c*TMH2 and the NEM- and $Ag^{+}$-sensitive residues of *a*TMH4. The proximal placement of *a*TMH4 next to the *c*-ring dictated by these cross-links might also suggest that *a*TMH5 is close to *c*TMH2. A proximal interaction had previously been suggested because the essential Arg-210 residue in *a*TMH4 could be replaced by an Arg in *a*TMH5 in the *a*R210Q/Q252R suppressor strain with partial retention of function (16, 23). The function of the suppressor strain clearly suggested that *c*Asp-61, *a*Arg-210, and *a*Gln-52 should pack proximally to each other in the membrane. However, zero-length cross-links between *a*TMH5 and *c*TMH2 were not identified in a previous survey of 32 Cys pairs.[3]

In this study we have attempted to determine the distance between *a*TMH5 and *c*TMH2 using bis-MTS reagents that react to insert variable length spacers between cross-linkable Cys pairs. The bis-MTS derivatives react preferentially with the ionized, thiolate form of the Cys side chain (24, 25). Cross-linking was attempted in 62 Cys substituted pairs in *a*TMH5 and *c*TMH2 and positive cross-links were observed in 12 cases. The lack of cross-linking for the 50 surrounding Cys-Cys pairs indicates the structural specificity of the cross-links formed. Cross-linking for most pairs was largely pH insensitive. However, certain cross-links demonstrated a pH dependence that would be consistent with *a*TMH5 rotating in response to acidification of the local environment. We suggest from these results that *a*TMH5 packs next to the *c*-ring and could play a role in gating $H^{+}$ transport to *c*Asp-61 in response to acidification of the periplasmic half-channel in $F_0$.

## EXPERIMENTAL PROCEDURES

*Construction of Cys-substituted Mutants*—Cys substitutions were initially introduced into subunit *a* or subunit *c* by a two-step PCR method using a synthetic oligonucleotide, which contained the codon change, and two wild type primers (26). To generate the double mutant, plasmids containing single Cys substitutions in subunit *a* were digested with HindIII and BsrGI, and the insert containing the subunit *a* mutation was ligated into the vector containing the subunit *c* mutation. All mutations were confirmed by sequencing through the ligation sites. In the initial screen for cross-linkable Cys pairs, the double Cys mutants were transferred into plasmid pDF163, which encodes subunits *a*, *b*, *c*, and δ, and transformed into strain JWP109 that carries a chromosomal deletion for the genes of these subunits (22). All of the double Cys substitutions showing positive cross-links were eventually transferred into plasmid pCMA113, which contains a $His_6$ tag on the C terminus of subunit *a* and an $F_1F_0$ where all native Cys have been substituted by Ala or Ser (18), and the biochemical characterization was carried out in this background. Each of the doubly Cys-substituted mutants grew on succinate minimal medium agar plates within the range of colony sizes seen for the singly substituted Cys mutants (20, 22, 27), *i.e.* 1.0–2.5 mm. The function of double Cys substitutions showing cross-linking was further evaluated by determining the growth yield on glucose and the capacity to pump protons as assessed by ATP-driven quenching of ACMA fluorescence (25).

*Membrane Preparation*—Inside-out membrane vesicles were prepared as follows. Plasmid transformant strains were grown in M63 minimal medium containing 0.6% glucose, 2 mg/liter thiamine, 0.2 mM uracil, 1 mM L-arginine, 0.02 mM dihydroxybenzoic acid, and 0.1 mg/ml ampicillin, supplemented with 10% LB medium, and harvested in the late exponential phase of growth (5). Cells were suspended in TMG buffer (50 mM Tris-HCl, 5 mM magnesium chloride, 10% glycerol, pH 8.5) containing 1 mM dithiothreitol, 1 mM phenylmethylsulfonyl fluoride, and 0.1 mg/ml DNase I and disrupted by passage through a French press at $1.38 \times 10^8$ newtons/$m^2$ and membranes prepared as described (28). The final membrane preparation was suspended in TMG buffer and stored at −80 °C. Protein concentrations were determined using a modified Lowry assay (28).

*Cross-linking with Bis-MTS Reagents*—Membranes of a mutant were diluted to 10 mg/ml in TMG buffer at pH 6.5, 7.5, or 8.5. The bis-MTS reagents were dissolved in dimethyl sulfoxide and added to the membranes to a final concentration of 2 mM. The reaction was incubated for 10 min at room temperature. The reaction was treated with 5 μl of 0.5 M $Na_2EDTA$, pH 8.0, and incubated at 37 °C for 15 min. βMSH was added to a final concentration of 4% by volume or alternatively DTT was added to a concentration of 20 mM to reduce the cross-link. The reduced samples were incubated at 37 °C for 15 min. Membranes were dissolved by addition of an equal volume of 2× SDS sample buffer (0.125 M Tris, 20% glycerol, 4% SDS, pH 6.8) before analyzing by SDS electrophoresis.

*Cross-linking with $Cu^{2+}$*—Membranes of a mutant were diluted to 10 mg/ml in TMG buffer at the indicated pH value. A 15 mM $CuSO_4$ and 45 mM *o*-phenanthroline solution was made in TMG at the same pH value as the membranes. Then, 5 μl of $Cu^{2+}$-phenanthroline solution was added to 50 μl (0.5 mg) of membranes to begin cross-linking. The reaction was incubated at room temperature for 1 h. The reaction was stopped by the addition of 5 μl of 0.5 M $Na_2EDTA$, pH 8.0, and was incubated at 37 °C for 15 min. To some samples βMSH was also added to a final concentration of 4% by volume. Membranes were dissolved by addition of an equal volume of 2× SDS sample buffer before analyzing by SDS electrophoresis.

[3] B. E. Schwem and R. H. Fillingame, unpublished data.

*SDS Electrophoresis and Immunoblotting*—Samples were run on 15% Bio-Rad Criterion® gels. The gels were run for 60–90 min at 200 volts. The protein was transferred to PVDF membrane paper by applying 75 volts for 1.5 h in Towbin buffer (0.192 M glycine, 0.025 M Tris, 20% MeOH) (29). Western blotting was performed by incubating with 5 mg/ml of GE® Blocking Agent in 1× PBS-Tween (137 mM NaCl, 6.5 mM $Na_2HPO_4$, 0.1% Tween 20) for 1 h at room temperature or alternatively overnight at 4 °C. Rabbit antiserum made to the first 10 amino acids of subunit *a* was pre-absorbed to membranes lacking $F_0$ to reduce immunoartifacts (30). The 1° antisera against subunit *a* was diluted 1:5,000 in 1× PBS-Tween with 2% bovine serum albumin and incubated with the PVDF membrane for 1 h at room temperature. Horseradish peroxidase-conjugated anti-rabbit 2° antibody was diluted 1:40,000 in 1× PBS-Tween and incubated with the PVDF membrane for 1 h at room temperature. The PVDF membrane was incubated for 4.5 min with equal volumes of SuperSignal West Pico Chemiluminescent Substrates (Pierce). The PVDF membrane was then exposed to film to visualize the protein.

*Purification of a–c Complexes*—Subunit *a* or the *a–c* dimer was purified using a method similar to that described (18). Samples were prepared as described above except 300 μl (3 mg) of membranes were used for each reaction and no EDTA was added at the end of the reaction. To the 300 μl of membranes, 10 μl of 62 mM bis-MTS reagent in dimethyl sulfoxide was added and the reaction incubated for 10 min at room temperature. Then, 660 μl of wash buffer (50 mM Tris, 0.3 M NaCl, 1% SDS, pH 8) and 40 μl of nickel-nitrilotriacetic acid-agarose beads (Qiagen) were added to each sample. The mixture was gently mixed on a rocker platform for 1 h at room temperature. The beads were harvested by centrifuging in a microcentrifuge for 7 s at a maximum of 10,000 rpm. The beads were washed twice with 1 ml of wash buffer. The protein was eluted from the beads with 100 μl of elution buffer (62.5 mM Tris, 10% glycerol, 20 mM $Na_2EDTA$, 2% SDS, pH 6.75). To reduce some samples, 50 μl of the eluted protein was moved to a new tube and 1 μl of 100% βMSH was added. Samples were analyzed by SDS electrophoresis.

## RESULTS

*Cross-linking between aTMH5 and cTMH2*—In a previous study from this laboratory, extensive $Cu^{2+}$-catalyzed cross-linking between Cys substitutions in *a*TMH4 and *c*TMH2 was observed over a span of 19 amino acid residues in the two TMHs (22). However, no cross-linking between Cys introduced into *a*TMH5 and the *c*TMH2 substitutions was observed with 32 double Cys substitutions using the same method.[4] These results suggest that *a*TMH4 may pack close to the periphery of the *c*-ring and that *a*TMH5 may pack at a greater distance. To investigate the proximity of *a*TMH5 to the *c*-ring, we utilized bis-MTS reagents with variable length spacers to probe for cross-linking in the current study (Fig. 1). The four reagents used in this study have a methanethiosulfonate moiety on both ends that reacts specifically with the thiolate form of a Cys side chain (24). These highly specific reagents have been used previously as "molecular rulers" to describe the packing of TMHs in P-glycoprotein (25), as perhaps the most definitive example.

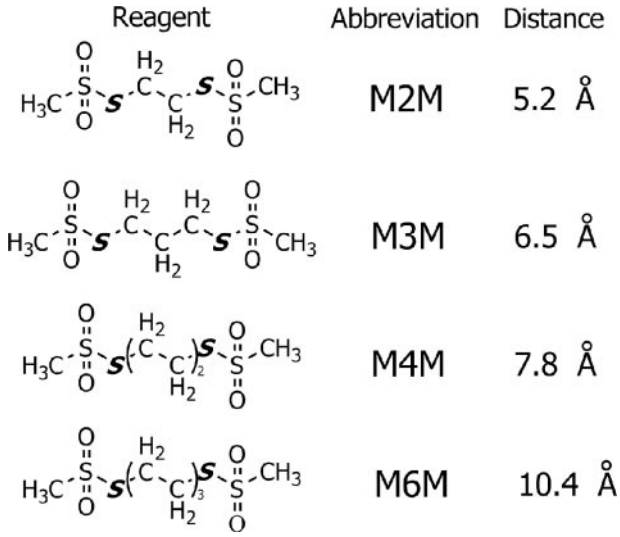


FIGURE 1. **Structure of the four bis-MTS reagents used in this study.** The theoretical distances between the sulfurs (*S*) forming disulfide bonds with Cys side chains is indicated (from Ref. 25).

Based upon the positive *a–c* cross-links formed with the *a*N214C and *c*A62C or *c*M65C in *c*TMH2 (22), and because an efficient intrasubunit *a* cross-link can be achieved between *a*G218C and *a*I248C (21), we initiated experiments assuming that *a*I248C might also be close to *c*TMH2. Initially, cross-linking was attempted from position *a*I248C in TMH5 of subunit *a* to positions *c*V60C, *c*A62C, *c*I63C, and *c*M65C in *c*TMH2. Nearly quantitative cross-linking was achieved for the *a*I248C/*c*A62C double Cys mutant when membranes were treated with any of the four bis-MTS reagents (Fig. 2*A*). Cross-linking was indicated by the appearance of a slower migrating band that is shown by experiments described below to correspond to an *a–c* dimer. The cross-link was largely reversed upon the addition of the reductant DTT. Because the linkers require the thiolate form of Cys for reaction, the pH of the buffer was varied to determine the effect of pH on the cross-link product formation. Surprisingly, there was no discernable decrease in cross-link formation upon lowering the pH from 8.5 to 6.5. Cross-link formation with the M4M and M6M reagents was incompletely and inconsistently reversed by DTT treatment at the lower pH values in this and several other experiments (Fig. 2*A*).

Limited cross-linking was obtained for the *a*I248C/*c*I63C double Cys mutant with M2M but higher yields were achieved with the longer linkers (Fig. 2*B*). Dimer formation increased to near 100% efficiency as the linker length was further increased with the M4M and M6M reagents (Fig. 2*B*). As with *a*I248C/*c*A62C, varying the pH in the range of 6.5 to 8.5 had no effect on the efficiency of cross-link formation. The cross-link was completely reversed by DTT treatment. Nearly 100% cross-linking was obtained for the *a*I248C/*c*M65C double Cys mutant with all four bis-MTS reagents (Fig. 2*C*). As with *a*I248C/*c*A62C and *a*I248C/*c*I63C, no effect on the cross-link formation was seen upon varying the pH. An immunoartifact band that migrates slower than the *a–c* dimer upon reduction with DTT was observed in this experiment and in other experiments with

[4] B. E. Schwem, unpublished data.

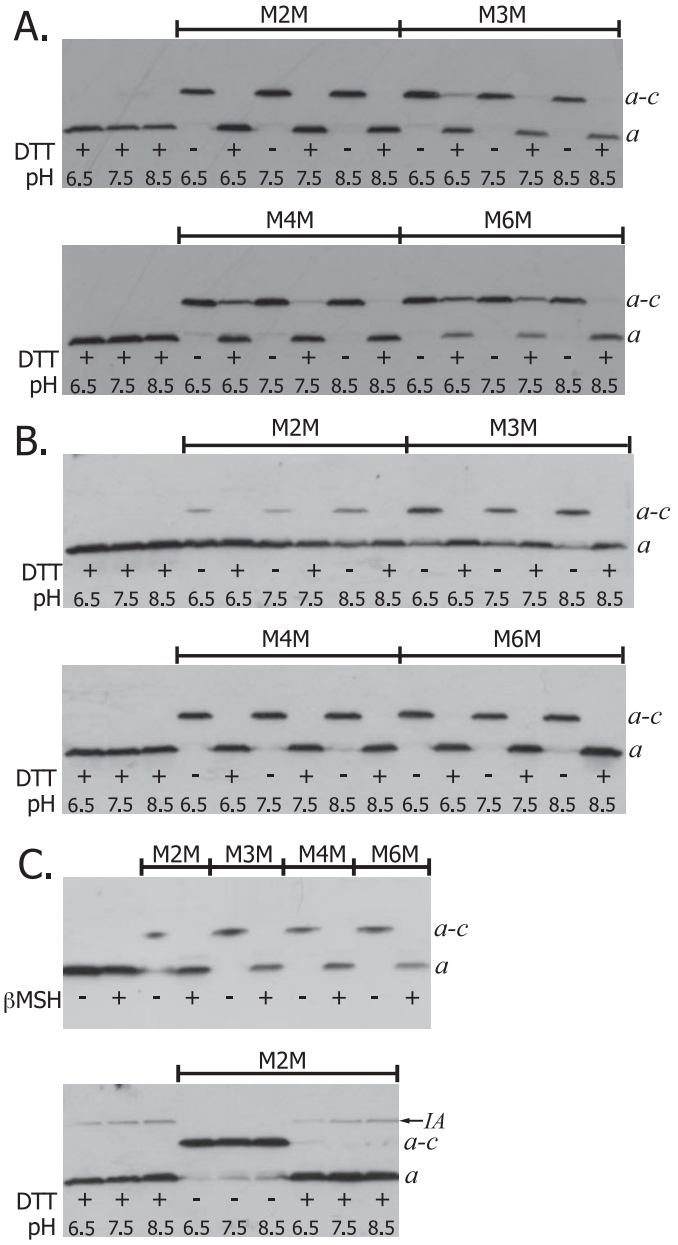


FIGURE 2. **Bis-MTS reagent catalyzed cross-link formation between Cys at position 248 in subunit *a* and at positions 62, 63, and 65 in subunit *c*.** Membranes were treated with the indicated bis-MTS reagent according "Experimental Procedures." The effect of pH on cross-link formation was determined by resuspending membrane pellets in TMG buffer at the indicated pH. Solubilized membranes were analyzed by SDS electrophoresis and Western blots were used to visualize subunit *a*. The bands corresponding to subunit *a* and the *a*–*c* dimer are indicated. *A*, *a*I248C/*c*A62C; *B*, *a*I248C/*c*I63C; and *C*, *a*I248C/*c*M65C. *IA* indicates immunoartifact.

βMSH reduction. This immunoartifact, marked *IA* in Fig. 2*C*, is occasionally seen and has greater intensity at higher pH values. The *a*I248C/*c*V60C double Cys mutant was not cross-linked with M2M, M4M, or M6M and indicated the specificity of cross-link formation for the *a*I248C/*c*A62C, *a*I248C/*c*I63C, and *a*I248C/*c*M65C mutants (Tables 1 and 2).

To ensure specificity of the cross-links at *a*I248C, Cys mutants were constructed and tested between residues on opposite sides of the proposed helices of *a*TMH5 and *c*TMH2. A total of 15 mutants were tested for cross-linking between residues *a*L247C, *a*I248C, *a*I249C, or *a*T250C to *c*M57C, *c*L59C, *c*V60C, *c*A62C, *c*I63C, or *c*M65C. All 18 of the tested mutants were negative indicating that the cross-links were confined to one side of *a*TMH5 and one side of *c*TMH2 (Table 1).

To verify the presence of both subunit *a* and subunit *c* in the proposed *a*–*c* dimer band, the His tag on subunit *a* was used to purify subunit *a* as described under "Experimental Procedures" before and after cross-linking. The purified protein from membranes of *a*I248C/*c*M65C treated with M2M exhibited two bands when analyzed by SDS-PAGE and Western blotting. Immunoblotting of the purified His-tagged subunit *a* or *a*–*c* products with antisera to both subunit *a* and subunit *c* separately confirmed that the lower band is non-cross-linked subunit *a* and the upper band is an *a*–*c* dimer (Fig. 3). When the purified, cross-linked products were treated with βMSH and probed with either antisera, one band was visible corresponding to either subunit *a* or subunit *c* (Fig. 3).

To continue the scan, Cys mutants were constructed and tested for cross-linking from *a*L251C to *c*M57C, *c*L59C, *c*V60C, *c*A62C, *c*I63C, and *c*M65C. The *a*L251C/*c*L59C double Cys mutant exhibited ~50% cross-linking efficiency with the M2M linker (Fig. 4*A*). The amount of dimer formation for *a*L251C/*c*L59C decreased considerably when mutant membranes were treated with the M4M and M6M reagents (Fig. 4*A*). The *a*L251C/*c*A62C double Cys mutant exhibited ~50% cross-linking efficiency with small linkers and greatly reduced cross-linking with M6M at pH 8.5 (Fig. 4*B*). The *a*L251C/*c*M57C pair showed 25% cross-linking with M2M at pH 8.5 and negligible cross-linking with the longer linkers (Table 2, and data not shown). Thus, unlike other cross-links identified in this study, the *a*L251C/*c*M57C, *a*L251C/*c*L59C, and *a*L251C/*c*A62C substitutions demonstrated a lower cross-linking efficiency with longer linkers. This could indicate that the space between the Cys pairs is limited and constrains the size of the linker. Cross-linking was not achieved between the *a*L251C and the *c*V60C, *c*I63C, or *c*M65C substitutions (Table 1). The M2M cross-linking of the *a*L251C/*c*L59C pair showed an unusual pH dependence where cross-link formation increased as the pH was decreased from 8.5 to 6.5 (Fig. 4*A*). The increase in cross-link formation with decreasing pH is less striking for the M4M and M6M linkers. A similar pH dependence with M2M was seen with the *a*L251C/*c*M57C substituted pair. Possible explanations for the pH dependence are discussed below.

*Cross-linking between aTMH5 and cTMH2 at the Cytoplasm*—To further define the interaction of *a*TMH5 with *c*TMH2, cross-linking was attempted between residues that are proposed to be located at the cytoplasmic side of the membrane. Cross-linking was attempted from *a*V262C to *c*R50C, *c*Q51C, *c*F53C, *c*F54C, *c*I55C, and *c*V56C. The *a*V262C/*c*I55C double Cys mutant cross-linked efficiently with bis-MTS reagents at a range of pH values (Fig. 5*A*). A high yield cross-link was also achieved with $Cu^{2+}$ at a range of pH values (Fig. 5*B*). The $Cu^{2+}$ cross-link with the 262/55 Cys pair was unique in that the other 11 bis-MTS cross-linkable Cys pairs reported in this study were not cross-linkable with $Cu^{2+}$ (data not shown). The *a*V262C/*c*F53C double Cys mutant exhibited 50–75% cross-link formation with all linkers and no cross-linking with $Cu^{2+}$ (Fig. 6*A*). The *a*V262C/*c*F54C double Cys mutant cross-linked efficiently

**TABLE 1**

**Cys pairs forming cross-links between *c*TMH2 and *a*TMH5 with M2 M at pH 8.5**

Symbols indicate: 0, no cross-link formed; + approximately 10–25% cross-link formation; ++ approximately 25–60% cross-link formation; +++ approximately 75% cross-link formation; ++++ approximately 90–100% cross-link formation.

| Subunit *c* | Subunit *a* | | | | | | | | | | |
|---|---|---|---|---|---|---|---|---|---|---|---|
| | Trp-241 | Phe-244 | Leu-247 | Ile-248 | Ile-249 | Thr-250 | Leu-251 | Gln-252 | Val-262 | Tyr-263 | Met-266 |
| Ala-39 | | | | | | | | | | | 0 |
| Ala-40 | | | | | | | | | | | 0 |
| Gln-42 | | | | | | | | | | | 0 |
| Pro-43 | | | | | | | | | | | 0 |
| Asp-44 | | | | | | | | | | | 0 |
| Arg-50 | | | | | | | | | 0 | 0 | |
| Thr-51 | | | | | | | | | 0 | 0 | |
| Phe-53 | | | | | | | | | ++ | 0 | |
| Phe-54 | | | | | | | | | ++++ | ++ | |
| Ile-55 | | | | | | | | | +++ | 0 | |
| Val-56 | | | | | | | | | 0 | 0 | |
| Met-57 | | | | 0 | 0 | 0 | + | | | | |
| Gly-58 | | | 0 | 0 | 0 | | | | | | |
| Leu-59 | | | | 0 | 0 | 0 | ++ | 0 | | | |
| Val-60 | | | 0 | 0 | 0 | 0 | 0 | 0 | | | |
| Ala-62 | | | 0 | ++++ | 0 | 0 | ++ | ++ | | | |
| Ile-63 | | | 0 | + | 0 | 0 | 0 | 0 | | | |
| Met-65 | | | | +++ | 0 | 0 | 0 | ++ | | | |
| Val-68 | 0 | 0 | | | | | | | | | |
| Gly-71 | 0 | | | | | | | | | | |
| Tyr-73 | | 0 | | | | | | | | | |
| Val-74 | 0 | | | | | | | | | | |
| Met-75 | 0 | | | | | | | | | | |
| Phe-76 | 0 | 0 | | | | | | | | | |
| Ala-77 | 0 | | | | | | | | | | |
| Val-78 | 0 | | | | | | | | | | |

**TABLE 2**

**Cys pairs forming cross-links between *a*TMH5 and *c*TMH2 using bis-MTS reagents of varying length**

Cross-linking at pH 8.5 was scored as in Table I.

| Mutant | M2M | M3M | M4M | M6M |
|---|---|---|---|---|
| 248/62 | ++++ | ++++ | ++++ | ++++ |
| 248/63 | + | ++ | ++++ | ++++ |
| 248/65 | +++ | ++++ | ++++ | ++++ |
| 251/57 | + | 0 | 0 | 0 |
| 251/59 | ++ | ++ | ++ | + |
| 251/62 | ++ | ++ | ++ | + |
| 252/62 | ++ | ++ | +++ | +++ |
| 252/65 | ++ | ++ | ++++ | ++++ |
| 262/53 | ++ | +++ | +++ | +++ |
| 262/54 | ++++ | ++++ | ++++ | ++++ |
| 262/55 | +++ | +++ | +++ | +++ |
| 263/54 | ++ | ++ | ++ | +++ |

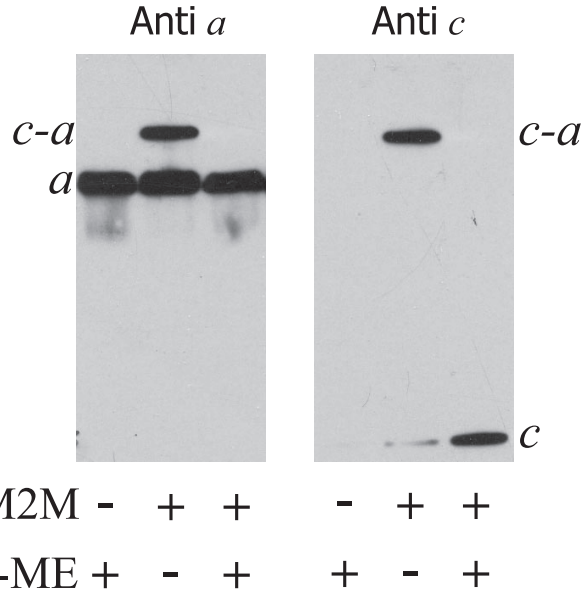


FIGURE 3. **Purified *a*–*c* dimer formed with M2M bis-MTS cross-linker.** Membranes of the mutant *a*I248C/*c*M65C were treated with M2M and His-tagged subunit *a* or *a*–*c* dimer was purified as described under "Experimental Procedures." A single gel was run with duplicate loading of samples to probe with both subunit *a* antibody and subunit *c* antibody. *β-ME*, mercaptoethanol.

with all bis-MTS reagents at pH 8.5 (Fig. 6*B*). The efficiency of cross-link formation was unaffected by varying the pH from 8.5 to 6.5 with both mutants (data not shown). The 3 double Cys mutants from residues *a*V262C to *c*R50C, *c*Q51C, or *c*V56C showed no cross-linking with any linker (Table 1).

*Cross-linking between aTMH5 and cTMH2 at the Periplasm*—Several attempts were made to cross-link between *a*TMH5 and *c*TMH2 at the periplasmic side of the membrane. A total of 10 mutants were tested. No cross-linking was achieved from *a*W241C to *c*V68C, *c*G71C, *c*V74C, *c*M75C, *c*F76C, *c*A77C, and *c*V78C (Table 1). In addition no cross-linking was achieved from *a*F244C to *c*V68C, *c*Y73C, and *c*F76C (Table 1). A possible reason for these negative results is inaccessibility to these residues to the bis-MTS reagents. In support of this possibility, the $Cu^{2+}$-catalyzed cross-linkable pairs *a*L224C/*c*Y73C, *a*I225C/*c*L72C, and *a*I225C/*c*Y73C identified previously (22) between *a*TMH4 and *c*TMH2 at the periplasmic side of the membrane were also resistant to forming dimers when treated with the M2M, M3M, M4M, and M6M linkers (data not shown). However, the 10 Cys pairs constructed here at the periplasmic side of *a*TMH5 and *c*TMH2 proved to be resistant to cross-linking with $Cu^{2+}$ at pH 8.5 (data not shown), so factors other than aqueous access may be responsible for the negative results.

*pH-dependent Cross-links*—As previously mentioned, the position of residue 252 in subunit *a* is of functionally significance because loss of the essential *a*Arg-210 residue in *a*TMH4 can be compensated in the double mutant suppressor strain *a*R210Q/Q252R (16, 23). To investigate the proximity of *a*Gln-

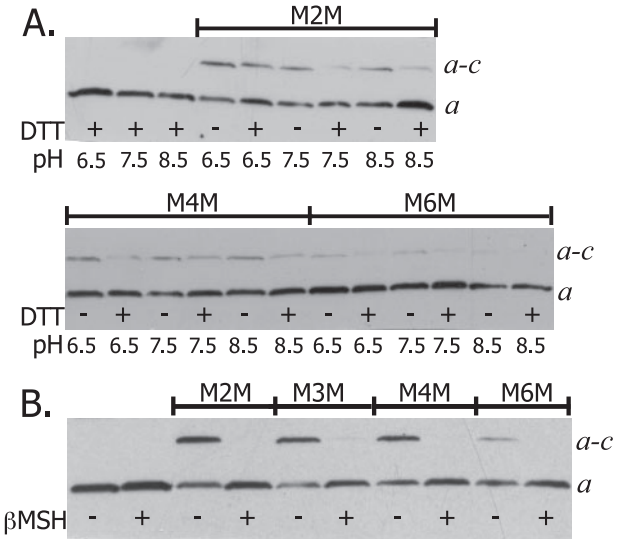


FIGURE 4. **Bis-MTS reagent catalyzed cross-link formation between Cys at position 251 in subunit *a* and positions 59 and 62 in subunit *c*.** Membranes were treated at the pH indicated in *A* or at pH 8.5 in *B*. Electrophoresis and Western blotting were carried out as described in the legend to Fig. 2. *A*, *a*L251C/*c*L59C; and *B*, *a*L251C/*c*A62C.

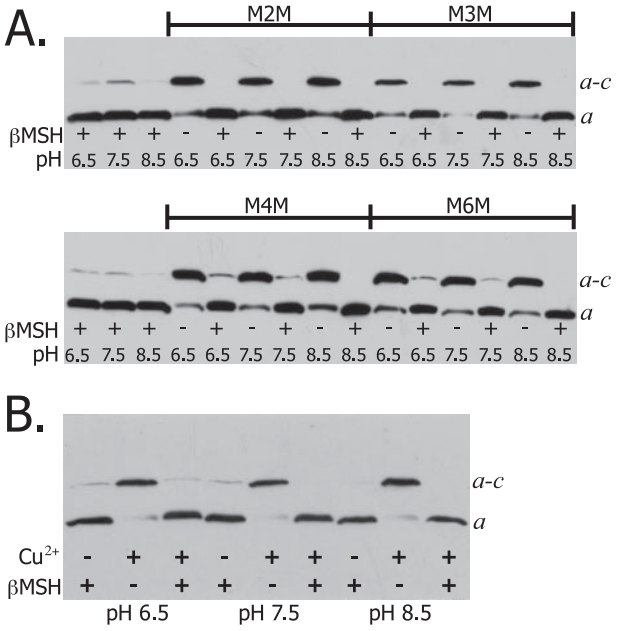


FIGURE 5. **Bis-MTS reagent and $Cu^{2+}$ catalyzed cross-link formation between Cys at position 262 in subunit *a* and position 55 in subunit *c* at various pH values.** *a*V262C/*c*I55C membranes were treated with *bis*-MTS (*A*) reagents or 1.5 mM $Cu^{2+}$-phenanthroline (*B*) as described under "Experimental Procedures." Electrophoresis and Western blotting were carried out as described in the legend to Fig. 2.

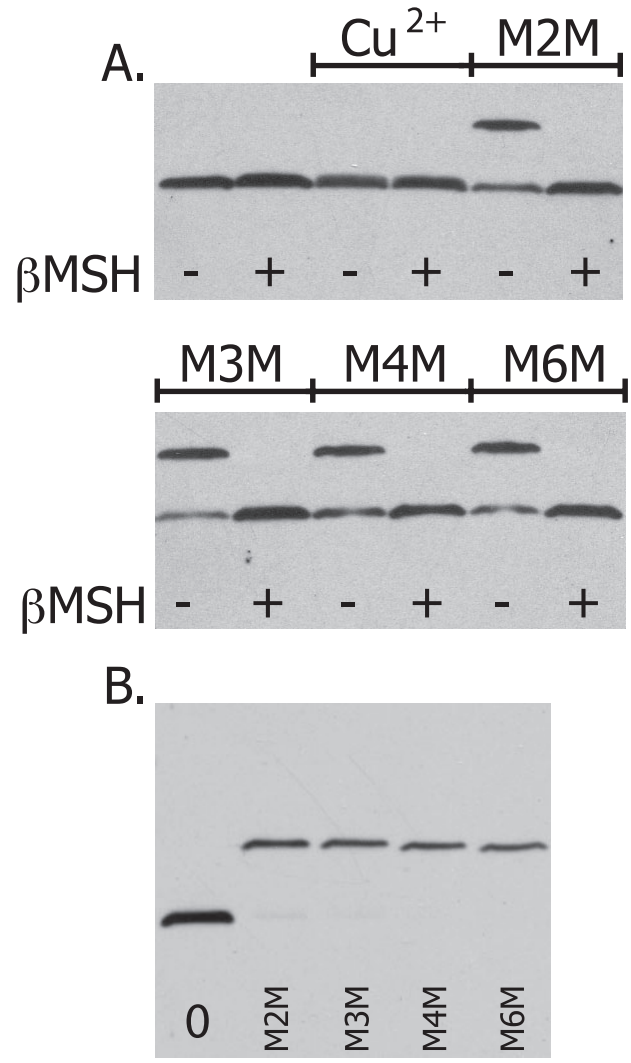


FIGURE 6. **Bis-MTS reagent catalyzed cross-link formation between Cys at position 262 in subunit *a* and positions 53 and 54 in subunit *c*.** Membranes were treated at pH 8.5 and electrophoresis and Western blotting were carried out as described in the legend to Fig. 2. *A*, *a*V262C/*c*F53C; and *B*, *a*V262C/*c*F54C.

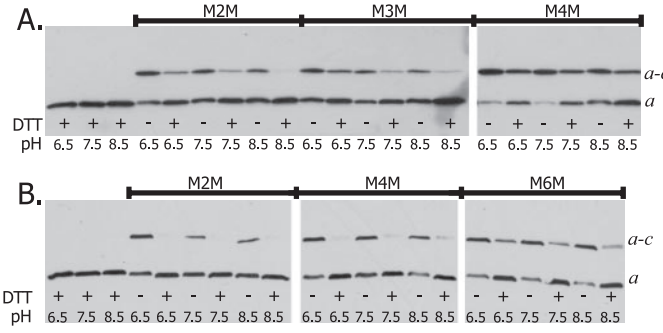


FIGURE 7. **pH-dependent cross-link formation between Cys at position 252 in subunit *a* and positions 62 and 65 in subunit *c* with *bis*-MTS reagents.** Membranes were treated and electrophoresis and Western blotting were carried out as described in the legend to Fig. 2. *A*, *a*Q252C/*c*A62C; and *B*, *a*Q252C/*c*M65C.

252 to *c*Asp-61, Cys mutants were constructed to test cross-linking between *a*Q252C and *c*L59C, *c*V60C, *c*A62C, *c*I63C, or *c*M65C. Cross-linking proved possible for two of the five mutant combinations.

The *a*Q252C/*c*A62C double Cys mutant cross-linked with M2M, M3M, and M4M linkers (Fig. 7*A*). When the pH was varied, treatment with the M2M linker generated noticeably more *a*–*c* dimer when the pH was lowered from 8.5 to 6.5 (Fig. 7*A*). A similar effect was seen with the M3M and M4M reagent (Fig. 7*A*). The increase in cross-linking at acidic pH was unusual in that, with the exception of the *a*L251C/*c*M57C and *a*L251C/*c*L59C pairs, other positive cross-linkable Cys pairs had shown no pH dependence with respect to cross-linking (Figs. 2 and 5). The *a*Q252C/*c*M65C double Cys mutant cross-

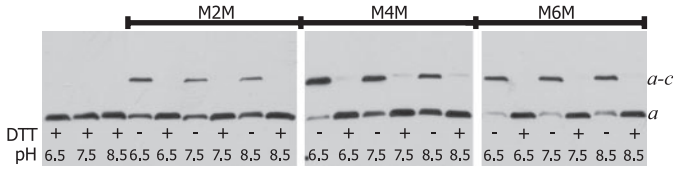


FIGURE 8. **pH-dependent cross-link formation between Cys at position 263 in subunit *a* and position 54 in subunit *c* with *bis*-MTS reagents.** *a*Y263C/*c*F54C membranes were treated and electrophoresis and Western blotting was carried out as described in the legend to Fig. 2.

linked with moderate product formation with the M2M and M4M reagents and greater than 75% product formation with the M6M reagent (Fig. 7*B*). As with the *a*Q252C/*c*A62C pair, product formation was increased when the pH was decreased from 8.5 to 6.5 (Fig. 7*B*).

Because the bis-MTS reagents react exclusively with the thiolate form of the Cys side chain, the cross-linked products shown in Fig. 7 would have been expected to decrease rather than increase at the lower pH. A possible explanation is that at acidic pH, *a*L251C and *a*Q252C of *a*TMH5 assume a position that is in closer proximity to *c*TMH2, which would allow for more efficient cross-linking at the lower pH values. To further investigate this and test a possible swiveling of the helix toward *c*TMH2, cross-linking was attempted between *a*Y263C and *c*R50C, *c*Q51C, *c*F53C, *c*F54C, *c*I55C, or *c*V56C. The *a*Tyr-263 residue was chosen based on its placement at the interior of the proposed four-helical bundle of subunit *a* along with *a*Gln-52 (21). Positive cross-links between *a*Y263C and any subunit *c* residue might also be sensitive to a conformational change brought about by lowering the pH. Of the 6 mutants tested, only the *a*Y263C/*c*F54C double Cys mutant demonstrated positive cross-linking with the M2M, M4M, and M6M cross-linkers (Fig. 8). The amount of cross-linked product increased as the pH was decreased from 8.5 to 6.5. The increase in cross-link formation at pH 6.5 was consistently most apparent for the M4M cross-linker, with only minor differences being seen in the extent of cross-linking with M2M and M6M (Fig. 8).

*aTMH4 and aTMH5 Can Be Cross-linked to Different Monomers*—Preliminary modeling of the cross-links identified in this study and in Jiang and Fillingame (22) suggested that *a*TMH4 and *a*TMH5 could be cross-linking to different subunit *c* monomers. The possibility that different subunit *c* monomers could be cross-linked to *a*TMH4 and *a*TMH5 was tested by combining cross-linkable pairs from *a*TMH4 to *c*TMH2 and from *a*TMH5 to *c*TMH2 in a single mutant strain and then testing for *c*—*a*–*c* trimer formation. A quadruple Cys mutant was generated that combines cross-linkable residues *a*L224C/*c*Y73C, which cross-links with $Cu^{2+}$ (22), and cross-linkable residues *a*V262C/*c*F54C, which cross-links with the bis-MTS reagents as shown above. These cross-links occur at the periplasmic and cytoplasmic sides of the membrane, respectively. When this quadruple Cys mutant was treated with $Cu^{2+}$, dimers were formed that were reduced upon the addition of βMSH (Fig. 9*A*). When mutant membranes were treated with M3M, the predicted *a*–*c* dimer was formed along with a minor amount of a second band that is identified as a *c*–*a*–*c* trimer in additional experiments below (Fig. 9*B*). Both the dimer and

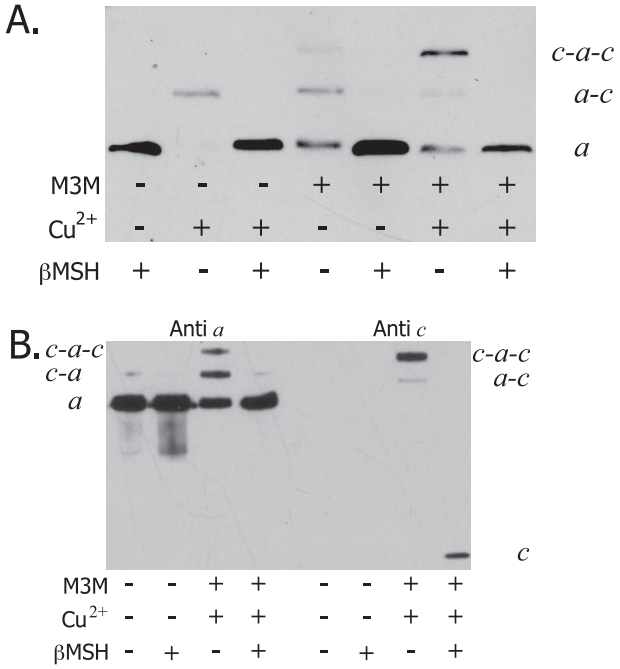


FIGURE 9. **A *c*—*a*–*c* trimer is formed by sequential treatment with M3M and $Cu^{2+}$.** *A*, membranes of the *a*L224C/*c*F54C and *a*V262C/*c*Y73C quadruple mutant were treated with $Cu^{2+}$, M3M, or both M3M and $Cu^{2+}$ to catalyze cross-link formation. *B*, the His-tagged subunit *a*, *a*–*c*, *or c*—*a*–*c* products were purified as described under "Experimental Procedures." A single gel was run with duplicate loading of samples to probe with both subunit *a* antibody and subunit *c* antibody as described in the legend to Fig. 3.

trimer complexes were reduced upon the addition of βMSH (Fig. 9*A*). When mutant membranes were treated sequentially with M3M and then $Cu^{2+}$, extensive *c*—*a*–*c* trimer formation was observed with the simultaneous disappearance of the *a*–*c* dimers (Fig. 9*A*). The presence of subunit *a* and subunit *c* in the cross-linked bands was verified by purifying the His-tagged subunit *a*, *a*—*c*, and *c*—*a*–*c* products before and after cross-linking (Fig. 9*B*). Antisera to both subunits *a* and *c* were used to visualize the individual subunits and the *a*–*c* and *c*—*a*–*c* products. The *a*–*c* product was consistently detected more readily by the anti-*a versus* anti-*c* antibodies in this and other experiments. These experiments demonstrate that *a*TMH4 and *a*TMH5 can be cross-linked to two different subunit *c* monomers.

*Function of Cross-linkable Double Cys Mutants*—The mutations used here could disrupt native structure, and if so, the cross-linking results described above would have to be evaluated with that consideration. The functional capacities of mutants showing positive cross-linking were assayed by measuring the growth yield in glucose minimal liquid medium, colony sizes on succinate minimal medium agar plates, and the ATP-driven $H^+$-pumping capacity (Table 3). Each of the doubly Cys substituted mutants grew on succinate minimal medium agar plates within the range of colony sizes seen for the singly substituted Cys mutants (20, 22, 27), *i.e.* 1.4–3.0 mm. Of the 12 double Cys mutants analyzed, 7 demonstrated growth yields on glucose that were ≥95% relative to wild type. Five mutants showed significantly lower growth yields. The capacity of each double Cys $F_1F_0$ to pump protons was assayed by ATP-driven quenching 9-amino-6-

**TABLE 3**
**Properties of subunit *a* and subunit *c* double Cys substitutions**

| *a*/*c* Mutation | Growth yield on glucose[a] | Growth on succinate[b] | % Quenching with ATP[c] |
|---|---|---|---|
| | | *mm* | |
| Wild type | 100 | 2.0–2.5 | 86 ± 3 |
| *a*I248C/*c*A62C | 100 | 2.2–3.0 | 65 ± 2 |
| *a*I248C/*c*I63C | 102 | 2.2–3.0 | 74 ± 1 |
| *a*I248C/*c*M65C | 81 | 1.8–2.0 | 51 ± 2 |
| *a*L251C/*c*M57C | 83 | 2.0–2.4 | 45 ± 7 |
| *a*L251C/*c*L59C | 71 | 1.5–2.0 | 35 ± 5 |
| *a*L251C/*c*A62C | 103 | 2.2–3.0 | 63 ± 6 |
| *a*Q252C | 92 | 1.8–2.2 | 54 ± 7 |
| *a*Q252C/*c*A62C | 77 | 1.5–2.0 | 12 ± 3 |
| *a*Q252C/*c*M65C | 68 | 1.4–1.8 | 11 ± 3 |
| *a*V262C/*c*F53C | 97 | 2.0–3.0 | 72 ± 2 |
| *a*V262C/*c*F54C | 96 | 2.0–3.0 | 34 ± 7 |
| *a*V262C/*c*I55C | 97 | 2.2–3.0 | 11 ± 2 |
| *a*Y263C/*c*F54C | 95 | 2.0–2.4 | 34 ± 1 |
| *a*L224C/*c*Y73C/ *a*Y263C/*c*F54C | 60 | <0.1 | ≤5 |

[a] Growth yield in liquid minimal media containing 0.04% glucose, expressed as a percentage of growth relative to the cysteine-less control. The values given are the average of two or more determinations. The growth yield of the *unc* deletion strain JWP292 was 59%.
[b] Colony size after incubation for 72 h on minimal medium plates containing 22 mM succinate. Colonies from the cysteine-less control strain show average colony sizes of 2.2 ± 0.3 mm.
[c] Membranes were diluted to 1 mg/ml in 10 mM Hepes-KOH, pH 7.5, 5 mM $MgCl_2$, 300 mM KCl for assay. The values given are the relative quenching 9-amino-6-chloro-2-methoxyacridine fluorescence following addition of ATP (±S.D. for two or more determinations).

chloro-2-methoxyacridine fluorescence. Of the 12 Cys mutants showing positive cross-linking, 9 mutants demonstrated relatively robust quenching responses in the range of the component singly substituted Cys (34–74%). Three double Cys mutants showed significantly reduced quenching responses in the range of 10–12%. The quadruple Cys mutant composed of cross-linkable pairs aL224C/cY73C with aV262C/cF54C formed small colonies of <0.1 mm on succinate and grew with a growth yield on glucose that was comparable with the *unc* deletion strain JWP292. The quadruple Cys mutant showed a negligible quenching response of ≤5%. The lack of function in this mutant could be due to a structural perturbation, or to the cumulative effects of the four Cys substitutions, each of which by themselves cause minor loss of function.

## DISCUSSION

Prior to this study, we reported that *a*TMH4 could be cross-linked to *c*TMH2 via $Cu^{2+}$-catalyzed disulfide bond formation over a span of 19 amino acids, which suggested that these helices packed in close proximity and possibly in parallel to each other (22). Zero-length cross-links generated with $Cu^{2+}$ were also used to define the packing of TMHs 2–5 of subunit *a* in what is likely a four-helix bundle (21). A model has been proposed placing the *a*TMH 2–5 four-helix bundle at the periphery of the *c*-ring with *c*TMH2 next to *a*TMH4, which suggested a possible close proximity of *a*TMH5 and *c*TMH2 (18). Such a proximity was supported by the function of the *a*R210Q/Q252R double mutant where the essential Arg of subunit *a* was exchanged between *a*TMH4 and *a*TMH5. The essential Arg is thought to interact with Asp-61 of *c*TMH2 during proton translocation. Despite the likely proximity, attempts to cross-link 32 pairs of Cys between *a*TMH5 and *c*TMH2 with $Cu^{2+}$ were unsuccessful.[3] In this study, we have used bis-MTS reagents to increase the distance and flexibility of a potential cross-link and have demonstrated cross-linking between *a*TMH5 and *c*TMH2 for 12 double Cys pairs. The specificity of cross-linking is demonstrated by the 50 pairs of Cys in neighboring residues that do not cross-link (Table 1). Nearly 100% cross-linking was obtained with various linkers for *a*I248C/*c*A62C, *a*I248C/*c*I63C, and *a*I248C/*c*M65C in the middle of the membrane and *a*V262C/*c*F54C and *a*V262C/*c*I55C at the cytoplasmic side of the membrane (Table 2). Slightly less efficient cross-linking was observed with the *a*L251C/*c*L59C, and *a*L251C/*c*A62C pairs at the center of the membrane and the *a*V262C/*c*F53C pair at the cytoplasmic surface (Table 2). The *a*V262C/*c*I55C mutant also formed dimers when treated with $Cu^{2+}$, whereas the other 11 cross-linkable pairs did not.

Several of the Cys pairs showed increasing cross-linking as the length of the linker was increased, *e.g.* *a*I248C/*c*I63C (Table 2), which is consistent with the side chains packing at a distance greater than that required for zero-length cross-linking with $Cu^{2+}$. The *a*L251C/*c*M57C, *a*L251C/*c*L59C, and *a*L251C/*c*A62C pairs were unusual in that cross-linking occurred most efficiently with the smallest cross-linkers, suggesting that the space between side chains may limit access of the cross-linking agent.

The structural modeling of the cross-linkable residues identified in this study and in Jiang and Fillingame (22) proves to be somewhat ambiguous because many cross-links could be depicted as occurring between *a*TMH4 or *a*TMH5 and two possible *c*TMH2s in the *c*-ring (Fig. 10). For example, Cys at positions 248 or 252 in *a*TMH5 could cross-link to Cys at positions 62 or 65 in either the *c*2′ or *c*2″ subunits shown in Fig. 10. On the other hand, the *a*I248C/*c*I63C cross-link seems much more probable with *c*2′ than with *c*2″. An attempt to limit the number of possible models that could be generated was made by combining cross-linkable pairs from *a*TMH4 to *c*TMH2 and from *a*TMH5 to *c*TMH2 in a quadruple Cys mutant. The Cys pairs *a*L224C/*c*Y73C and *a*V262C/*c*F54C cross-link specifically with $Cu^{2+}$ and bis-MTS reagents, respectively, to cause *a*–*c* dimer formation. When membranes were treated sequentially with both reagents, two cross-links were formed from subunit *a* to two separate subunit *c* monomers generating a *c*–*a*–*c* trimer. This verified that *a*TMH4 and *a*TMH5 can cross-link to different subunit *c* monomers. A possible model consistent with these results is shown in Fig. 10 where *a*TMH4 cross-links with the *c*2″ and the *c*2‴ subunits and *a*TMH5 within the same subunit *a* cross-links with the *c*2′ and *c*2″ subunits. The model needs to be considered with caution because the quadruple mutant used in direct support proved to be nonfunctional, and the loss of function therein could result from disruption of the normal *a*–*c* structural interaction.

Five cross-linkable Cys pairs, *i.e.* *a*L251C/*c*M57C, *a*L251C/*c*L59C, *a*Q252C/*c*A62C, *a*Q252C/*c*M65C, and *a*Y263C/*c*F54C, showed pH-dependent cross-linking where cross-link formation was increased by decreasing the pH from 8.5 to 6.5. This pH dependence was opposite to expectations because one would predict that cross-linking should decrease at more acid pH because the Cys thiolate is the reactive species (24). For the

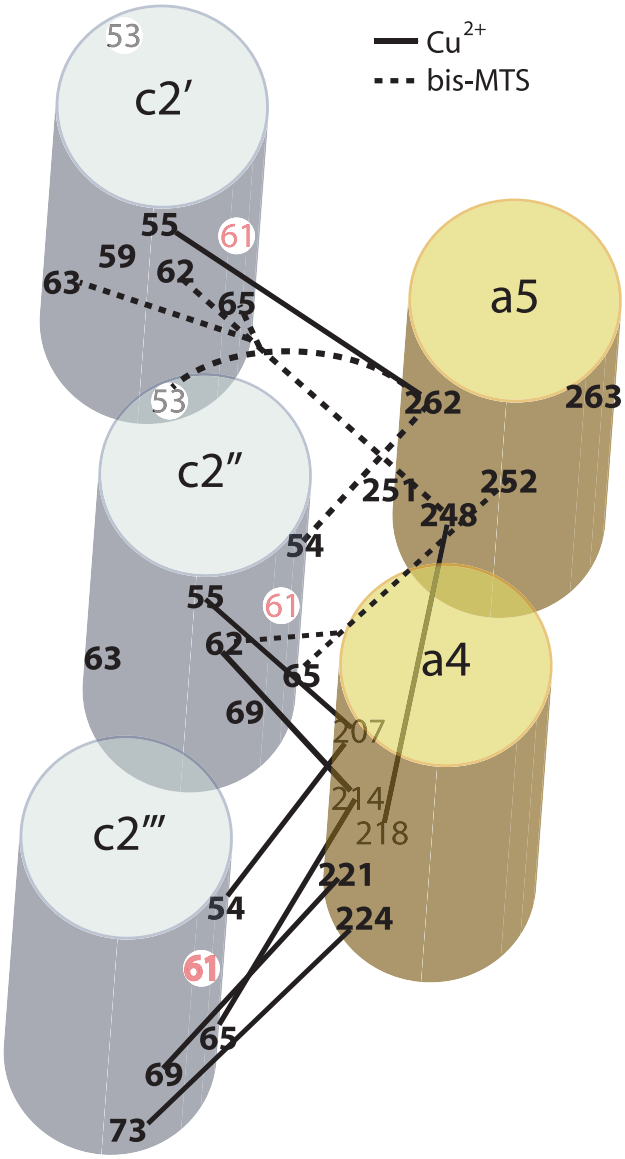


FIGURE 10. **Schematic representation of TMH4 and TMH5 of subunit *a* docked next to three copies of TMH2 of subunit *c* based on available cross-linking data.** *a*TMH4 and *a*TMH5 (*yellow cylinders*) were placed next to three identically oriented copies of *c*TMH2, the *c*TMH2 orientation being based upon the *I. tartaricus* x-ray structure (7). Residues involved in cross-linking in this study and Jiang and Fillingame (22) are indicated. The schematic illustrates how the helices might pack next to subunit *c* and indicate one possible means by which *a*TMH5 and *a*TMH4 interact with different *c*TMH2s. The helices are assumed to pack in parallel. *a*TMH4 and *a*TMH5 are oriented relative to each other based upon the *a*G218C/I248C zero-length cross-link catalyzed by $Cu^{2+}$-phenanthroline (21).

other seven Cys pairs, cross-linking did not change over the range of pH 6.5–8.5 (Figs. 2 and 5, and data not shown for the *a*L251C/*c*A62C, *a*V262C/*c*F53C, and *a*V262C/*c*F54C Cys pairs). All of the pH-dependent, cross-linkable mutants exhibited at least partial function as reflected by growth on glucose and succinate carbon sources and by ATP-driven $H^+$-pumping, although function did vary considerably (Table 3). The retention of partial function in these mutants suggests that the key structural interactions at the subunit *a*–*c* interface of these mutants are likely to be largely preserved.

We have suggested previously that TMHs 4 and 5 may rotate in response to acidification of the periplasmic half-channel that is thought to be located at the center of the four-helix bundle of TMHs 2–5 (14, 19–21). The movements were proposed as part of a gating mechanism to allow for protonation of the *c*Asp-61 from the periplasm during proton translocation. During ATP synthesis, Asp-61 in *c*TMH2 must sequentially undergo protonation and deprotonation. Arg-210 in *a*TMH4 is proposed to interact with *c*Asp-61 to lower its $pK_a$ to promote proton release. Following deprotonation, all or part of *a*TMH4 could rotate counterclockwise to move *a*Arg-210 away from *c*Asp-61 to facilitate its reprotonation, and with the simultaneous rotation of *a*TMH5 clockwise, gate access to protons at the interior of the four-helix bundle to facilitate reprotonation from the periplasm. Based upon the model shown in Fig. 10, a clockwise rotation of *a*TMH5 would bring *a*Gln-52 and *a*Tyr-263 closer to *c*TMH2. This could explain why cross-linking is increased in the mutants involving these residues when the pH is lowered. A local pH change at the interior of the four-helix bundle on the reduction of the medium pH from 8.5 to 6.5 could cause *a*TMH5 to rotate as postulated from other studies (14, 20).

*Acknowledgment—We thank Hun Sun Chung for assistance in some of the experiments.*

## REFERENCES

1. Yoshida, M., Muneyuki, E., and Hisabori, T. (2001) *Nat. Rev. Mol. Cell. Biol.* **2,** 669–677
2. Capaldi, R. A., and Aggeler, R. (2002) *Trends Biochem. Sci.* **27,** 154–160
3. Dimroth, P., von Ballmoos, C., and Meier, T. (2006) *EMBO Rep.* **7,** 276–282
4. Senior, A. E. (1988) *Physiol. Rev.* **68,** 177–231
5. Jiang, W., Hermolin, J., and Fillingame, R. H. (2001) *Proc. Natl. Acad. Sci. U. S. A.* **98,** 4966–4971
6. Mitome, N., Suzuki, T., Hayashi, S., and Yoshida, M. (2004) *Proc. Natl. Acad. Sci. U. S. A.* **101,** 12159–12164
7. Meier, T., Polzer, P., Diederichs, K., Welte, W., and Dimroth, P. (2005) *Science* **308,** 659–662
8. Pogoryelov, D., Yu, J., Meier, T., Vonck, J., Dimroth, P., and Muller, D. J. (2005) *EMBO Rep.* **6,** 1040–1044
9. Jones, P. C., Jiang, W., and Fillingame, R. H. (1998) *J. Biol. Chem.* **273,** 17178–17185
10. Dmitriev, O. Y., Jones, P. C., and Fillingame, R. H. (1999) *Proc. Natl. Acad. Sci. U. S. A.* **96,** 7785–7790
11. Valiyaveetil, F. I., and Fillingame, R. H. (1998) *J. Biol. Chem.* **273,** 16241–16247
12. Long, J. C., Wang, S., and Vik, S. B. (1998) *J. Biol. Chem.* **273,** 16235–16240
13. Wada, T., Long, J. C., Zhang, D., and Vik, S. B. (1999) *J. Biol. Chem.* **274,** 17353–17357
14. Fillingame, R. H., Angevine, C. M., and Dmitriev, O. Y. (2003) *FEBS Lett.* **555,** 29–34
15. Cain, B. D. (2000) *J. Bioenerg. Biomembr.* **32,** 365–371
16. Hatch, L. P., Cox, G. B., and Howitt, S. M. (1995) *J. Biol. Chem.* **270,** 29407–29412
17. Valiyaveetil, F. I., and Fillingame, R. H. (1997) *J. Biol. Chem.* **272,** 32635–32641
18. Angevine, C. M., and Fillingame, R. H. (2003) *J. Biol. Chem.* **278,** 6066–6074
19. Angevine, C. M., Herold, K. A., and Fillingame, R. H. (2003) *Proc. Natl. Acad. Sci. U. S. A.* **100,** 13179–13183
20. Angevine, C. M., Herold, K. A., Vincent, O. D., and Fillingame, R. H. (2007) *J. Biol. Chem.* **282,** 9001–9007
21. Schwem, B. E., and Fillingame, R. H. (2006) *J. Biol. Chem.* **281,** 37861–37867

22. Jiang, W., and Fillingame, R. H. (1998) *Proc. Natl. Acad. Sci. U. S. A.* **95,** 6607–6612
23. Ishmukhametov, R. R., Pond, J. B., Al-Huqail, A., Galkin, M. A., and Vik, S. B. (2008) *Biochim. Biophys. Acta* **1777,** 32–38
24. Roberts, D. D., Lewis, S. D., Ballou, D. P., Olson, S. T., and Shafer, J. A. (1986) *Biochemistry* **25,** 5595–5601
25. Loo, T. W., and Clarke, D. M. (2001) *J. Biol. Chem.* **276,** 36877–36880
26. Barik, S. (1996) *Methods Mol. Biol.* **57,** 203–215
27. Steed, P. R., and Fillingame, R. H. (2008) *J. Biol. Chem.* **283,** 12365–12372
28. Mosher, M. E., White, L. K., Hermolin, J., and Fillingame, R. H. (1985) *J. Biol. Chem.* **260,** 4807–4814
29. Towbin, H., Staehelin, T., and Gordon, J. (1979) *Proc. Natl. Acad. Sci. U. S. A.* **76,** 4350–4354
30. Hermolin, J., and Fillingame, R. H. (1995) *J. Biol. Chem.* **270,** 2815–2817